Nanoscale Advances

ROYAL SOCIETY OF CHEMISTRY

PAPER

View Article Online
View Journal | View Issue



Cite this: *Nanoscale Adv.*, 2025, **7**, 3732

# Green synthesis and characterization of *Blumea sinuata* silver nanoparticles: antibacterial, antifungal, and antioxidant properties†

Umakant Pradhan, [a] Jagdish Prasad Prajapati, [b] Purusottam Majhi, [a] Dibyasha Sahu,[b] Rajesh Kumar Singh, [c] Sadhucharan Mallick [b] and Awadhesh Kumar Shukla *[a]

The plant *Blumea sinuata* (Lour.) Merr. harbours high amounts of phytoconstituents, some of which have strong reduction and capping potential. Eco-friendly and nontoxic silver nanoparticles have been synthesized using the plant extract of *B. sinuata*. The formation of *B. sinuata* silver nanoparticles (BS-$Ag_2O$ NPs) was confirmed through various techniques. UV-visible spectroscopy revealed an absorbance band at 408 nm, Fourier transform infrared spectroscopy (FTIR spectroscopy) identified functional groups serving as stabilizing and capping agents, essential for the formation of silver nanoparticles, dynamic light scattering (DLS) measurement indicated that the nanoparticles had a mean hydrodynamic diameter of 102.50 nm, and the evaluated zeta potential for surface charge analysis of BS-$Ag_2O$ NPs was found to be −16.4 mV. High-resolution transmission electron microscopy (HRTEM) showed an average particle size of 7.98 nm, and X-ray diffraction (XRD) analysis confirmed the face-centred cubic (FCC) structure of $Ag_2O$ NPs. The antibacterial activity of BS-$Ag_2O$ NPs against phytopathogenic bacteria *Erwinia carotovora*, *Ralstonia solanacearum*, and *Xanthomonas oryzae* was assessed by the agar-well diffusion method. At 400 μg concentration of BS $Ag_2O$ NPs, the maximum zones of inhibition were 20.66 mm and 20.33 mm against *E. carotovora* and *R. solanacearum*, respectively. While a zone of inhibition of 14.33 mm was observed against *X. oryzae*. Biogenic BS-$Ag_2O$ NPs exhibited remarkable antifungal activity against phytopathogenic fungi, namely *Alternaria alternata*, *Aspergillus niger*, *Aspergillus flavus*, and *Fusarium oxysporum*. At a concentration of 1.5 mg $mL^{-1}$ BS-$Ag_2O$ NPs, the percentage of inhibition was 91.70, 62.65, 58.96, and 50.45 on the growth of *A. alternata*, *A. flavus*, *A. niger*, and *F. oxysporum*, respectively. The antioxidant activity of BS-$Ag_2O$ NPs was evaluated by 2,2-diphenyl-1-picrylhydrazyl hydrate (DPPH) as well as 2,2-azino-bis(3-ethylbenzothiazoline-6-sulfonic acid) (ABTS) methods. The reported DPPH free radical scavenging activity was 25.85 ± 0.36% at 80 μg $mL^{-1}$ concentration of BS-$Ag_2O$ NPs, and in the case of ABTS, it was found to be 40.28% at 80 μg $mL^{-1}$ concentration of BS-$Ag_2O$ NPs.

Received 23rd December 2024
Accepted 20th April 2025

DOI: 10.1039/d4na01063a

rsc.li/nanoscale-advances



## 1. Introduction

Over the past twenty years, nanotechnology has progressed into one of the most hastily advancing areas of scientific research. With its distinctive qualities and broad applications across various areas, including medicine, food, and agriculture, as well as in industries, nanotechnology has become one of the most significant and attractive subjects of study.[1,2] Nanoparticles exhibit different properties to bulk particles. The small size of nanoparticles with a high surface area, as well as versatile optical, magnetic, mechanical, and chemical characteristics, make them suitable for biological applications.[3,4] They demonstrate potential roles as antimicrobials, antioxidants, anticancer agents, and antibiotics.[5,6]

Green nanotechnology is an emerging discipline for the development of nanomaterials and nanoproducts in ways that are safe for the environment and sustainable practise. This necessitates addressing the environmental and health concerns associated with conventional nanotechnology, which often involves toxic chemicals and hazardous waste.[7] The objective of green nanotechnology is to reduce the ecological impact of nanomaterial production and use by utilizing the green chemistry principle, thereby ensuring that the advantages of nanotechnology are realized without compromising environmental integrity.[8] For instance, the development of biodegradable

[a]*Microbiology Laboratory, Department of Botany, Indira Gandhi National Tribal University, Amarkantak 484887, India. E-mail: awadhesh.shukla@igntu.ac.in*

[b]*Nanomaterials Research Laboratory, Department of Chemistry, Indira Gandhi National Tribal University, Amarkantak 484887, India*

[c]*Department of Dravyaguna, Institute of Medical Science, Banaras Hindu University, Varanasi 221005, India*

† Electronic supplementary information (ESI) available. See DOI: https://doi.org/10.1039/d4na01063a

nanoparticles for drug delivery can be facilitated by green nanotechnology, thereby decreasing the effects of medical waste.[9] In the agriculture field, they can enhance the efficiency of pesticides and fertilizers, thereby minimising soil contamination and chemical discharge.[10]

Nanoparticles of silver (Ag), copper (Cu), gold (Au), and platinum (Pt) are commonly used in medical and biological fields because of their multipurpose theragnostic properties.[11,12] The synthesis of these noble metal NPs involves various methods, such as thermal decomposition[13], sono-chemical methods,[14] photochemical reactions in reverse micelles,[15] microwave-assisted processes,[16] hydrothermal methods,[17] co-precipitation methods,[18] *etc.* However, these synthesis processes typically require high temperatures and the use of hazardous chemicals along with expensive materials such as sodium borohydride, hydrazine hydrate, 2-mercaptoethanol, citrate, *etc.* Therefore, employing biological methods with microorganisms such as yeast, fungi, bacteria, viruses, and actinomycetes, along with utilizing plant extracts, offers a safe, money-making, and environmentally friendly alternative process.[7,19–21] The synthesis of nanoparticles using microorganisms is more intricate due to specific procedures like isolation, culture maintenance, and numerous purification stages. In contrast, NPs synthesized from plant extracts present more advantages over those produced intracellularly using microbes.[20] Due to these benefits, there has been a notable surge in attention, motivating researchers to develop environmentally friendly techniques utilizing numerous phytochemicals, such as leaves, peels, fruits, flowers, and roots.[8,22] Various phytoconstituents are present in the plant extract, including carbohydrates, ascorbic acid, flavonoids, terpenoids, polyphenols, *etc.*, which play crucial roles in reducing the metal ions and acting as capping agents.[23,24]

Silver nanoparticles exhibit an extensive range of applications, including anticancer, antimicrobial, and antiradical agents.[1,25] Various biosynthesis methods for silver-based nanoparticles have been documented in the published studies. For instance, Mussin *et al.* (2021)[26] used an aqueous extract of the plant *Acanthospermum australe* to effectively synthesise Ag NPs, showcasing both cytotoxic and antibacterial properties. Liaqat *et al.* (2022)[27] employed a combination of *Eucalyptus camaldulensis* and *Terminalia arjuna* plant extracts for the synthesis of Ag NPs and investigated their cytotoxicity and antimicrobial activities through hemolysis assays. Sobhani *et al.* (2016)[28] utilized a precipitation method to synthesize AgO nanostructures, studying their photocatalytic degradation of rhodamine B under visible light irradiation. Messaoudi *et al.* (2023)[29] achieved the green synthesis of $Ag_2O$ nanoparticles using the *Punica granatum* leaf extract for adsorption of sulfamethoxazole antibiotic.

Barwant *et al.* (2022)[19] successfully green-synthesized $Ag_2O$ NPs using *Solanum elaeagnifolium* and studied their antioxidant activity; they showed DPPH scavenging activity of 20.86% at 89.88 μg $mL^{-1}$ and ABTS scavenging activity of 25.75% at 85 μg $mL^{-1}$. Shirazi *et al.* (2022)[30] achieved the bio-fabrication of $Ag_2O$ NPs using *Mentha pulegium* and *Ficus carica* and checked their antibacterial activity at 50 mg $mL^{-1}$ concentrations. *M. pulegium* $Ag_2O$ NPs showed inhibition zones of 10 ± 0.53 (*Staphylococcus aureus*), 13 ± 0.10 (*Bacillus subtilis*), and 13 ± 0.32 mm (*Pseudomonas aeruginosa*), while *F. carica* $Ag_2O$ NPs exhibited inhibition zones of 12 ± 0.58 mm, 12 ± 0.29 mm, and 13 ± 0.62 mm against the same bacteria. Mahlambi *et al.* (2022)[3] synthesised starch-mediated green $Ag_2O$ NPs and evaluated their bactericidal activity. The NPs showed inhibition zones of 15 ± 0.19 against *S. aureus* and 14 ± 0.11 mm against *Escherichia coli* at 6 mg $mL^{-1}$ concentration.

*Blumea*, a member of the Asteraceae family, is recognized for its enormous number of phytochemical substances, typically attaining a height between 20 and 180 cm, and featuring an upright, often branched stem with a taproot and characterized by its hairy texture.[31] The plant is found to produce flower heads in large, open panicles at the terminations of its branches.[32] Noteworthy is the fact that this marks the inaugural instance of synthesizing silver nanoparticles from the *Blumea sinuata* plant. We know that there are no earlier reports on *B. sinuata* plant-based Ag and $Ag_2O$ NP synthesis. Numerous studies have explored the biological synthesis of $Ag_2O$ NPs using various plant extracts; however, a survey of the literature revealed that phytochemical constituent analysis of the plant extract and biogenic synthesis of silver nanoparticles using the *B. sinuata* plant extract has not yet been done. Investigations have also been not carried out on the antimicrobial activity of BS-$Ag_2O$ NPs. This work investigates the utilisation of BS-$Ag_2O$ NPs, revealing their potential as a new biocontrol agent for sustainable plant disease management.

This experimental study details the green production of silver nanoparticles utilising the watery plant extract of *B. sinuata* and investigation of their antimicrobial activity against various phytopathogenic bacteria and fungi and also antioxidant activity.

## 2. Experimental section

### 2.1. Materials and methods

The chemical reagents utilised in this experiment were of analytical grade and unpurified. Silver nitrate ($AgNO_3$, MW: 169.87 g $mol^{-1}$), 1,1-diphenyl 2-picrylhydrazyl (DPPH) and 2,2-azino-bis(3-ethylbenzothiazoline-6-sulfonic acid) (ABTS) were purchased from the Merck Chemicals; de-ionized water of Milli-Q grade and ciprofloxacin (HiMedia) were used; the phytopathogenic Gram-negative bacteria *E. carotovora* (BL0010), *R. solanacearum* (BI0004), and *X. oryzae* (BB0013) were obtained from The Indian Agricultural Research Institute, New Delhi. The National Culture Collection of Pathogenic Fungi (NCCPF), Department of Medical Microbiology, Chandigarh, India, provided phyto-pathogenic fungal cultures of *A. alternata*, *A. niger*, *A. flavus*, and *F. oxysporum*. The fungi were cultured on potato dextrose agar medium (HiMedia, Mumbai, India). The bacteria were cultured on Luria Agar medium (HiMedia, Mumbai, India).

### 2.2. Preparation of BS plant extract

Healthy and disease-free *B. sinuata* plants were collected from the Indira Gandhi National Tribal University (IGNTU) campus

in Amarkantak, Madhya Pradesh, India. The plant taxonomist from the Botany Department verified the identification. A sample voucher was placed at the departmental herbarium, and the assigned accession number was IGNTU/DOB/2024/Ast/Bs/01. Both regular tap water and deionised water were used to wash the collected plants. The plant material was air-dried at room temperature in the shade and later ground into a powder form. Around 10 g of crushed plant powder was mixed with 100 mL of distilled water in a 250 mL beaker. An aqueous plant extract was obtained by subjecting the mixture to a 45-minute heating process at 70 °C and then filtering it using Whatman no. 1 filter paper. This process was followed by qualitative phytochemical analysis and the production of BS-$Ag_2O$ NPs.

### 2.3. Phytochemical analysis

To determine phytochemical components in the water-based *B. sinuata* plant extract, a qualitative analysis was carried out. Phytochemical analysis of the leaf extract was carried out by the method suggested by Agidew *et al.* (2022)[23] and Flores-Bocanegra *et al.* (2025).[24] The phytochemical screening of the *B. sinuata* aqueous plant extract showed outstanding secondary metabolite content (Table 1).

### 2.4. Synthesis of BS-$Ag_2O$ NPs

An aqueous solution of 20 mM $AgNO_3$ solution was prepared by dissolving $AgNO_3$ in 100 mL of distilled water at room temperature. Thereafter, $AgNO_3$ solution was stored in an amber bottle. Next, 80 mL of the aqueous plant extract was transferred to a 250 mL beaker and stirred using a magnetic stirrer at room temperature. Subsequently, 20 mL of 20 mM (67.948 mg) $AgNO_3$ solution was added drop by drop to the stirred aqueous plant extract solution at pH 7. The overall reaction mixture was continuously stirred for 24 hours. Following that, a noticeable colour change from deep green to dark brown occurred, indicating the formation of $Ag_2O$ NPs. The dark brown reaction mixture was then centrifuged at 8000 rpm for 10 minutes, and the resulting pellet was washed three times using 70% ethanol. The collected pellet was dried at room temperature and further utilized for the characterization and study of antimicrobial activity and antioxidant properties (Fig. 1).

### 2.5. Characterization of nanoparticles

The synthesized BS-$Ag_2O$ NPs were subjected to UV-visible spectroscopy (Shimadzu, UV-1800). The synthesis of nanoparticles was carried out using 20 mL volume of 20 mM concentration of $AgNO_3$ with 80 mL of aqueous plant extract, followed by stirring at room temperature. In the process of stirring the solution, silver nitrate was added drop by drop until it showed a colour change, and subsequently scanning was done through a UV-visible spectrophotometer at wavelengths from 200 to 700 nm; the results showed a prominent peak at 408 nm, which confirmed the surface plasmon resonance observed in $Ag_2O$ NPs. FTIR (Thermo Scientific iDZ7 ATR, Nicolet iS5) in the 400–4000 $cm^{-1}$ range was utilized to investigate functional groups involved in reducing $AgNO_3$ to BS-$Ag_2O$ NPs. In the FTIR study, the number of scans was set to 16, and the resolution was 1 $cm^{-1}$. XRD studies (PANalytical, X'Pert3 powder X-ray diffractometer) were utilized to obtain the diffraction pattern of BS-$Ag_2O$ NPs with Cu $K_\alpha$ radiation. Dynamic light scattering (DLS) (Anton Paar Litesizer 500) methods have been used to investigate the hydrodynamic size, polydispersity index, and surface zeta potential of the synthesized BS-$Ag_2O$ NPs for surface charge analysis of $Ag_2O$, which will indicate the stability and rate of aggregation of $Ag_2O$ NPs. The particle size and morphology of BS-$Ag_2O$ NPs were measured using HRTEM (NEOARM/JEM-ARM200F JEOL). For TEM analysis of synthesized BS-$Ag_2O$ NPs, initially, nanoparticles were dispersed in an appropriate aqueous solution (5 μL) and ultrasonicated to prevent agglomeration, then for grid preparation a drop of the biologically synthesized BS-$Ag_2O$ NPs was dispersed onto a TEM grid (carbon coated copper grid) and allowed to completely dry for further processes. EDS analysis was done for obtaining the elemental composition of biologically synthesized BS-$Ag_2O$ NPs, for which an electron beam was focused on the specific area of interest and EDS spectra were acquired. However, selected area electron diffraction (SAED) analysis was performed by aligning the selected area with the electron beam and determining the crystal structure and phase identification of biologically synthesized BS-$Ag_2O$ NPs.

### 2.6. Antibacterial activity

The antibacterial efficacy of biologically synthesized BS-$Ag_2O$ NPs was assessed using the agar well diffusion method

Table 1 Phytochemical analysis of the aqueous *B. sinuata* plant extract

| S. no | Phytochemicals | Tests | Result |
|---|---|---|---|
| 1 | Tannins | Ferric chloride test | +ve |
| 2 | Saponins | Foam test | −ve |
| 3 | Flavonoids | Sodium hydroxide test | +ve |
| 4 | Glycosides | Chloroform and 10% ammonia solution test | −ve |
| 5 | Quinones | Sulphuric acid test | +ve |
| 6 | Phenol | Ferric chloride test | +ve |
| 7 | Terpenoids | Chloroform and conc. sulphuric acid test | +ve |
| 8 | Coumarins | Sodium hydroxide test | +ve |
| 9 | Cardiac glycosides | Ferric chloride test | +ve |
| 10 | Anthraquinones | Ammonia test | +ve |
| 11 | Steroids | Sulphuric acid test | +ve |
| 12 | Alkaloids | Mayer's reagent test | −ve |
| 13 | Phlobatannins | Hydrochloric acid test | −ve |

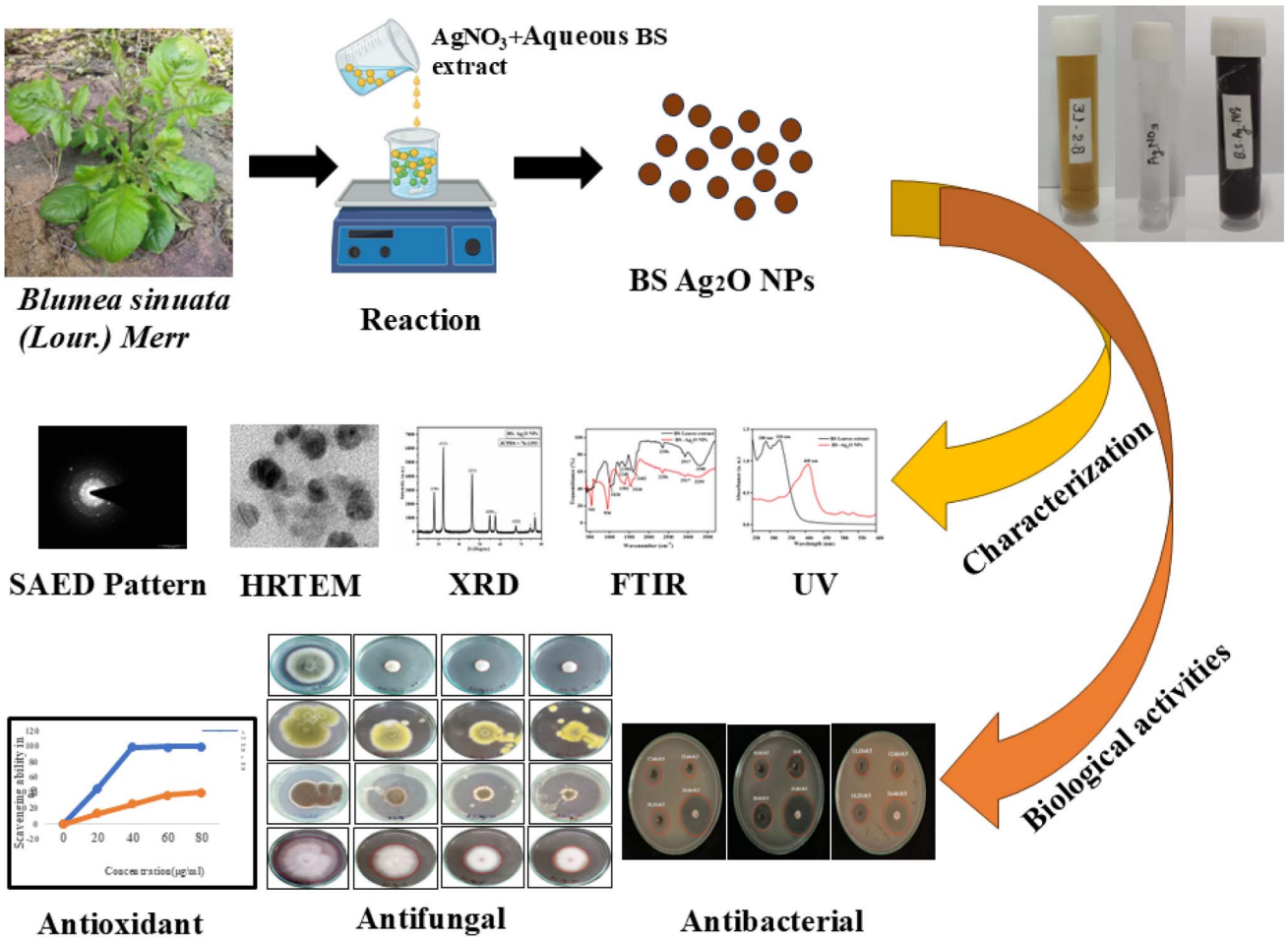


Fig. 1 Formation of BS-$Ag_2O$ NPs using the *B. sinuata* plant extract, characterization of BS-$Ag_2O$ NPs and biological activities assay of BS-$Ag_2O$ NPs.

suggested by Gomathi *et al.* (2020).[1] The phytopathogenic Gram-negative bacteria, *E. carotovora* (BL0010), *R. solanacearum* (BI0004), and *X. oryzae* (BB0013), were selected to measure the antibacterial activity of nanoparticles. These bacterial strains were sourced from the Indian Agricultural Research Institute, New Delhi. Initially, sterile Luria-Bertani (LB) agar was poured into plates and allowed to solidify for 10 minutes. Subsequently, an overnight bacterial culture was spread onto the agar plates using a cell spreader loop. Wells with a diameter of 5 mm were carefully created using a steel cork borer. After preliminary assessment, three different concentrations of 200, 300, and 400 μg $mL^{-1}$ BS-$Ag_2O$ NPs were loaded into three separate wells. As a control, a 5 μg ciprofloxacin disc (HiMedia) was included in the experiment. The plates were then incubated in a bacteriological incubator at 37 °C for 24–48 hours. Following the incubation period, the zones of inhibition were measured.

### 2.7. Antifungal activity studies

The antifungal activity of the biologically synthesized BS-$Ag_2O$ NPs was evaluated using the poisoned food technique.[33–35] The four phytopathogenic fungi, namely *A. alternata*, *A. niger*, *A. flavus*, and *F. oxysporum*, were obtained from the National Culture Collection of Pathogenic Fungi (NCCPF), Department of Medical Microbiology, Chandigarh, India. Three different concentrations (0.5 mg $mL^{-1}$, 1 mg $mL^{-1}$, and 1.5 mg $mL^{-1}$) of BS-$Ag_2O$ NPs were prepared in 5% dimethyl sulfoxide (DMSO). Using a sterile stainless-steel cork borer, 5 mm discs of pathogenic fungi (*A. alternata*, *A. niger*, *A. flavus*, and *F. oxysporum*) were placed in the centre of plates and temperature was maintained at 25 °C. After an incubation of 7 days, the zones of inhibition were measured. The calculation for the average percentage inhibition of mycelial growth was determined using formula (1) as follows:

$$\text{Average \% inhibition of mycelial growth} = \frac{(d_c - d_t)}{d_c} \times 100 \quad (1)$$

where $d_c$ is the average growth of fungal colony in control plates and $d_t$ is the average growth of fungal colony in treated plates.

### 2.8. Antioxidant activity of BS-$Ag_2O$ NPs

By using the DPPH and ABTS radical scavenging tests, the *in vitro* antioxidant activity of BS-$Ag_2O$ NPs was examined. The BS-$Ag_2O$ NPs and standard solution (ascorbic acid) concentrations used were 20, 40, 60, 80 and 100 μg $mL^{-1}$. To prevent

nanoparticle agglomeration, the colloidal suspension of BS-$Ag_2O$ NPs was sonicated for 30 minutes in a sonicator bath while the temperature was kept at room temperature. The absorbance was measured spectrophotometrically against a blank solution.[36,37]

The percentage inhibition was calculated using formula (2) as follows:

$$\text{Scavenged}(\%) = \frac{A_{\text{control}} - A_{\text{test/standard}}}{A_{\text{control}}} \times 100 \quad (2)$$

**2.8.1. DPPH.** The free radical scavenging ability of BS-$Ag_2O$ NPs was assessed using the 2,2-diphenyl-1-picrylhydrazyl (DPPH) technique.[38] Different concentrations (20–80 μg $mL^{-1}$) of biosynthesized $Ag_2O$ NPs were added to tubes containing 0.004 mM methanolic DPPH solution, and after 30 minutes of incubation in the dark, absorbance was measured at 517 nm. Ascorbic acid served as the standard chemical.[38,39]

**2.8.2. ABTS.** An amount of 192 mg of 2,2-azino-bis(3-ethylbenzothiazoline-6-sulfonic acid) (ABTS) was mixed with 50 mL of distilled water to make a 7 mM solution, and 2.45 mM potassium persulphate (32 mg in 50 mL) was added (1 : 1). Before use, the reaction mixture was left to stand for 24–48 h under dark conditions at room temperature. Different concentrations of samples and standards (0.2 mL) were mixed with freshly prepared BS-$Ag_2O$ NPs and 2.98 mL of ABTS solution. After 20 minutes, spectrophotometry was used to measure the absorbance at 734 nm.

# 3. Results and discussion

## 3.1. Structural and morphological analysis of BS-$Ag_2O$ NPs

On the basis of different methods such as UV-vis spectrophotometry, FTIR, XRD, TEM, and TEM-EDS, structural and morphological analysis of BS-$Ag_2O$ NPs was carried out. UV-visible spectroscopy was employed to analyze the absorption spectra of biogenically synthesized aqueous solution of BS-$Ag_2O$ NPs, focusing on the prominent peak at 408 nm attributable to the surface plasmon resonance (SPR) phenomenon observed in $Ag_2O$ NPs. Additionally, the BS plant extract exhibited absorption peaks at 288 nm and 328 nm, indicative of the presence of phytochemicals that contribute to the stabilization and formation of $Ag_2O$ NPs. In the biofabrication process of $Ag_2O$ NPs, various plant phytochemicals serve distinct roles; there are phytochemicals that are widely involved in bioreduction, such as phenolic compounds, flavonoids, alkaloids, terpenoids and vitamins, while some of them act as capping and stabilizing agents for nanoparticles, including proteins, polysaccharides, amino acids, polyphenols and, saponins. When silver nitrate solution is mixed with different phytochemicals, the phytochemicals act as reducing agent donating electrons to the silver ions ($Ag^+$) and reducing them to silver atoms (AgO), this process forms silver nanoparticles, once the silver NPs are formed, they can undergo controlled oxidation under suitable conditions. This oxidation converts the surface layer of Ag (0) and $Ag_2O$ NPs. This component helps in the formulation process to achieve $Ag_2O$ NPs with the desired size, shape and stability. Phytochemical screening of the aqueous plant extract of *B. sinuata* shows that it is an excellent source of secondary metabolites, as given in Table 1. Most of the phytochemicals that are extracted from plants in polar solvents are polar by nature and are important for the production of NPs.[40,41]

FTIR was employed to analyze the functional groups present in both the BS plant extract and BS-$Ag_2O$ NPs. In the FTIR study, the number of scans was set to 16 and the resolution was 1 $cm^{-1}$. The vibrational frequencies were examined, and notable peaks were identified. The O–H stretching band exhibited a vibration frequency of 3300–3250 $cm^{-1}$, while the C–H stretching bands of the methyl group were observed at 2917 $cm^{-1}$. The O=C=O stretching band manifested at a vibration frequency of 2356 $cm^{-1}$. Additionally, the amine's N–H bending mode was observed as a vibration band at 1602 $cm^{-1}$, and the N–O stretching band of the nitro group appeared at 1530 $cm^{-1}$. The O–H bending mode of phenol, C–N stretching mode of amine, and C–O stretching bands were observed at the vibration frequencies of 1384–1383 $cm^{-1}$, 1248 $cm^{-1}$, and 1030 $cm^{-1}$, respectively. The stretching bands associated with the Ag–O–Ag bond and Ag–O bond were identified at vibration frequencies of 950 $cm^{-1}$ and 541 $cm^{-1}$, respectively.[42]

DLS measurement shown in Fig. 3a indicates that BS-$Ag_2O$ NPs have a mean hydrodynamic diameter of 102.50 nm. A polydispersity index of 25.7% was obtained. Zeta potential is a key indicator of the long-term stability of BS-$Ag_2O$ NPs and is a critical aspect of their application in various biological applications, including antibacterial, antifungal, and antioxidant activity. Ensuring stability involves understating and controlling factors that influence physical and biological long-term stability. The evaluated zeta potential values of BS-$Ag_2O$ NPs in Fig. 3b were found to be −16.4 mV with a standard deviation of 0.3 mV. It depends on the motion of NPs under an electric field and the particle's surface charge.

The XRD pattern of the powder sample of biologically synthesized BS-$Ag_2O$ NPs is illustrated in Fig. 2C. The diffraction angles, corresponding to 2$\theta$ values, were observed at 27.93°, 32.32°, 46.35°, 54.94°, 57.55°, and 74.55°, aligning with the *hkl* values of (110), (111), (211), (220), and (221), (123) planes of $Ag_2O$ NPs, respectively. Additionally, 2$\theta$ values of 46.16°, 67.58°, and 77.04° align with the *hkl* values of (200), (220) and (311) planes of Ag NPs, respectively. The XRD results indicate that a trace amount of Ag(0) is present on the surface of $Ag_2O$ NPs. These values closely match the standard data file JCPDS-76-1393 and are consistent with the values in earlier reports on $Ag_2O$ NPs.[25] The discerned diffraction pattern strongly indicates the crystalline nature and cubic structure of $Ag_2O$ NPs.[41,43] The average crystallite size was determined using the Scherrer equation as follows:

$$(D = 0.9\ \lambda/\beta \cos\theta), \quad (3)$$

where $D$ represents the average crystallite size, $\lambda$ is the X-ray wavelength ($\lambda$ = 1.54 Å), $\beta$ is the full width at half-maximum (FWHM), and $\theta$ is the Bragg diffraction angle. The calculated mean average crystallite size of BS-$Ag_2O$ NPs is 22.96 nm.

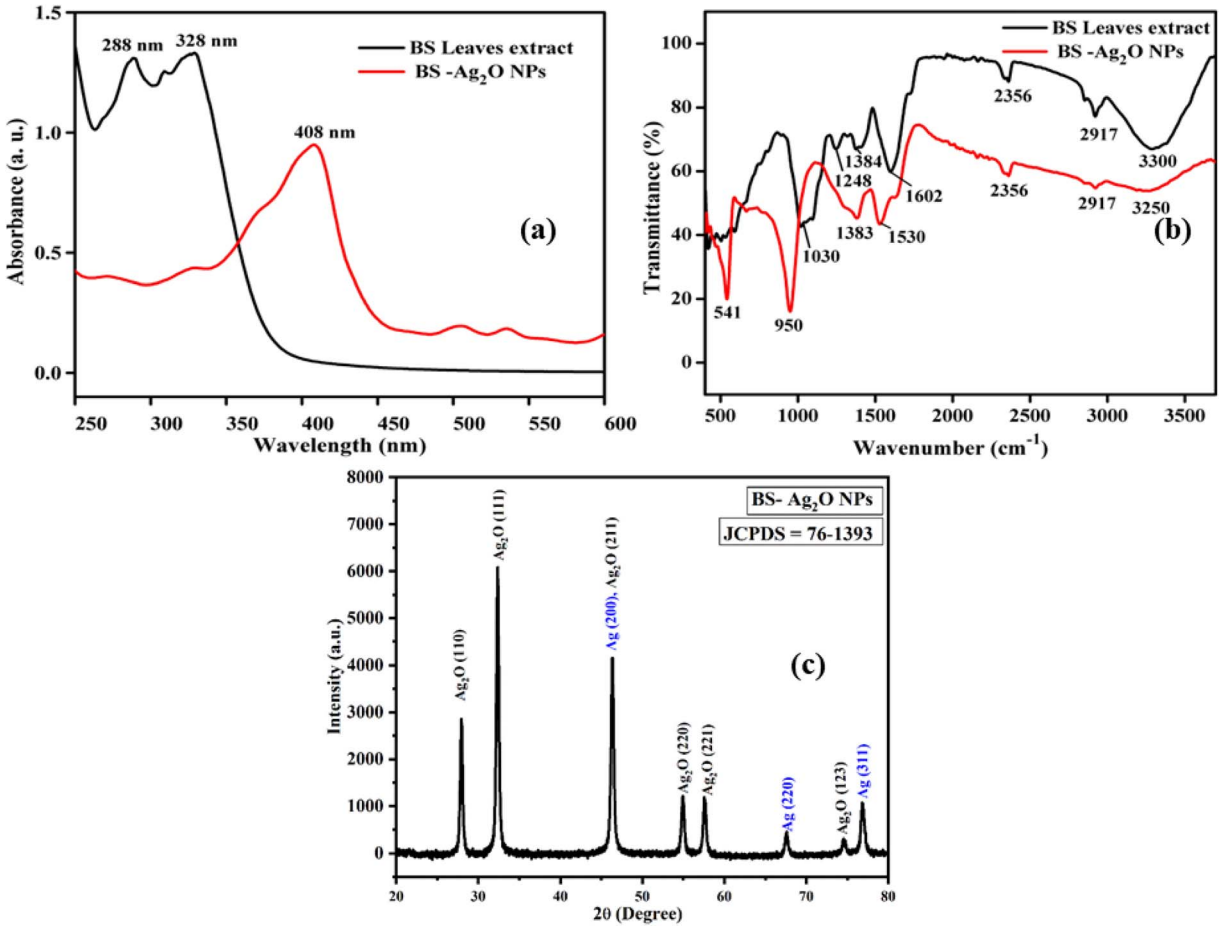


Fig. 2 (a) UV-visible spectra of BS-$Ag_2O$ NPs (red line) and BS plant extract (black line). (b) FTIR spectra of BS-$Ag_2O$ NPs (red line) and dry BS-leaf powder (black line). (c) XRD pattern of BS-$Ag_2O$ NPs.

Fig. 4 presents low- to high-resolution TEM images of biologically synthesized BS-$Ag_2O$ NPs. The TEM images reveal a nearly spherical structure, and the use of a histogram plot for size estimation indicates a range between 3.24 and 14.36 nm and an average particle size of 7.98 nm. Fig. 5a indicates the selected area electron diffraction (SAED) pattern that provides evidence of the polycrystalline nature of the BS-$Ag_2O$ NPs. Four different planes (111), (220), (211), and (123) were identified, which are consistent with the XRD pattern. Moreover, TEM-EDS spectra (Fig. 5b) focused on BS-$Ag_2O$ NPs show the occurrence of Ag and O elements in the corresponding sample. The inset shows the corresponding EDS result, presented in the form of a table. C peaks also confirm the presence of phytochemical constituents in BS-$Ag_2O$ NPs. As per the methods of protocol, a carbon-coated copper TEM grid that is being employed as a supporting material for the BS-$Ag_2O$ NPs sample is the source of the Cu peaks.

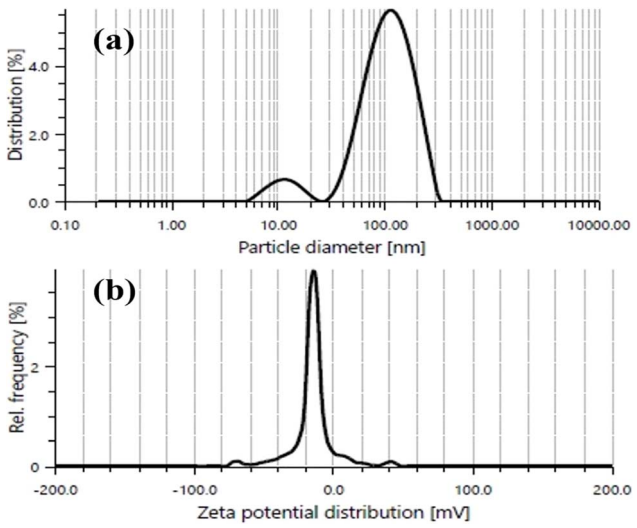


Fig. 3 (a) Graphical view of size and PDI properties of BS-$Ag_2O$ NPs. (b) Zeta potential of BS-$Ag_2O$ NPs.

### 3.2. Antibacterial effect of BS-$Ag_2O$ NPs

The impact of NPs was observed against three phytopathogenic bacteria, namely, *E. carotovora*, *R. solanacearum*, and *X. oryzae*. The results show that NPs have greater antibacterial activity against *E. carotovora* and *R. solanacearum* as compared to *X. oryzae*. At 400 μg $mL^{-1}$ concentration of BS-$Ag_2O$ NPs, inhibition zones recorded for *E. carotovora* and *R. solanacearum* are 20.66 mm and 20.33 mm, respectively. Whereas at the same

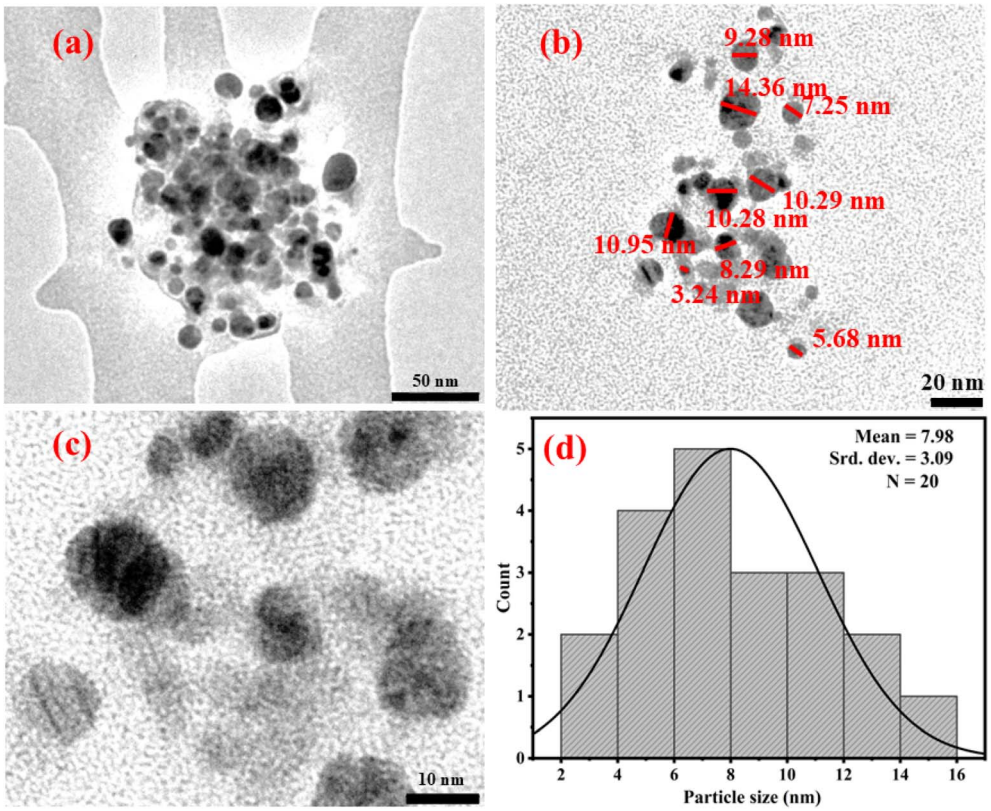


Fig. 4 (a–c) HR-TEM image (d) particle size distribution pattern of BS-$Ag_2O$ NPs.

concentration, inhibition zone for *X. oryzae* was 14.33 mm (Fig. 6 and 7). The proposed mechanism for BS-$Ag_2O$ NPs against *E. carotovora*, *R. solanacearum*, and *X. oryzae* may be that nanoparticles penetrate the cell membrane, producing physical damage and disrupting the membrane structure.[44] The disturbance results in the increase of the cell membrane permeability, causing protein leakage, which in turn results in irreversible membrane damage, membrane disintegration, and the entry of Ag NPs, which can alter the DNA replication mechanism, induce aberrant morphology, and ultimately cause cell death.[45] Silver nanoparticles have the ability to enter both the mitochondrial and cell membranes, resulting in structural damage and decreased adenosine triphosphate synthesis. Nanoparticles also interfere with bacterial metabolism and enzymatic activity by attaching to thiol groups, interrupting critical cellular function. Fig. 8 illustrates the possible mechanism underlying this enhanced antibacterial activity of BS-$Ag_2O$ NPs as their interactions with bacterial cells. The bacterial pathogen causes several diseases in vegetative crop plants by forming the bacterial soft rot on the onion (*E. carotovora*), bacterial wilt (*R. solanacearum*), and bacterial blight on rice (*X. oryzae*). Abbas *et al.* (2019) synthesized AgNPs, *i.e.* Ag, AgP, AgIB, AgAE, and AgBE, and evaluated their antibacterial activity against phytopathogenic bacteria *E. carotovora* and *E. atroseptica*.[46] Javed *et al.* (2020) green synthesized colloidal AgNPs and elicited their antibacterial activity against phytopathogenic bacterial strains,

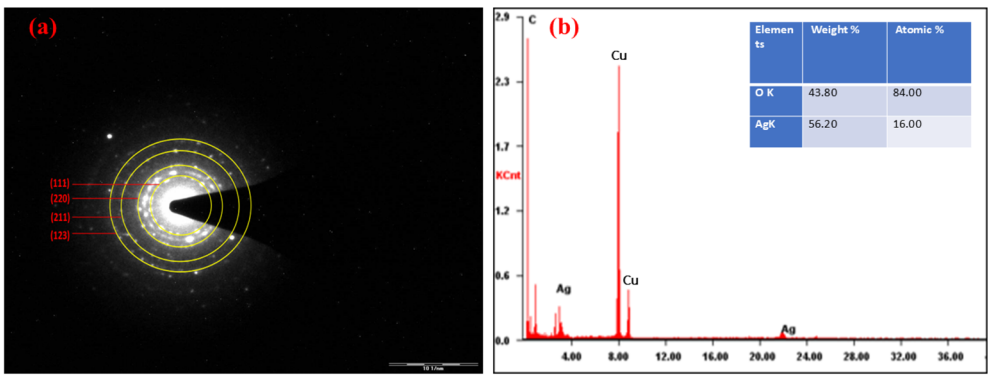


Fig. 5 (a) Selected area electron diffraction (SAED) and (b) TEM-EDS spectra of nanoparticles.

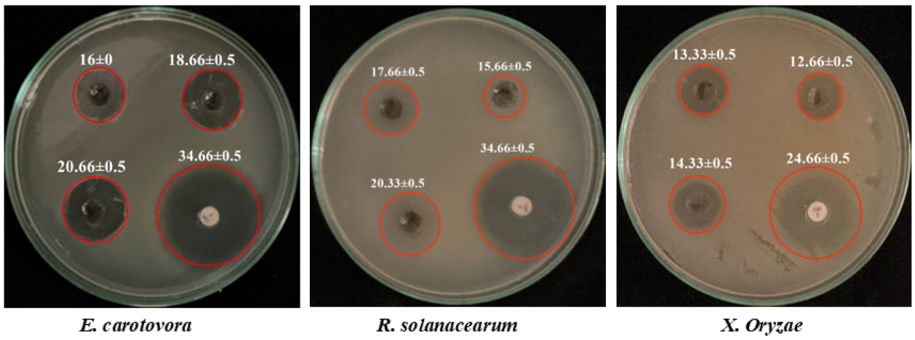


Fig. 6 Antibacterial activity of BS-$Ag_2O$ NPs against phytopathogenic bacteria.

*Pectobacterium carotovora*, *X. oryzae*, *X. vesicatoria* and *R. solanacearum*.[47] Dilbar *et al.* (2023) synthesized Ag NPs using the *Salvia nubicola* extract and evaluated their antibacterial activity against *R. solanacearum*.[48] It is an established fact that plant diseases reduce agricultural production; a large amount of money is found to be invested in plant disease management. Various types of chemicals are applied for crop protection; the use of chemical pesticides harms the environment, deteriorates human health, and destroys the habitat of different organisms that share the same niche. Therefore, alternative methods, including the use of green-synthesized Ag NPs for disease management, maybe a more viable and eco-friendly method.

### 3.3. Antifungal activity of BS-$Ag_2O$ NPs

The antifungal efficacy of BS-$Ag_2O$ NPs was assessed by determining the percentage of inhibition in the mycelial growth of selected fungi. The impact of BS-$Ag_2O$ NPs on the mycelial growth of all four fungi was found to be inhibitory, and the results indicate fungitoxicity against *A. alternata*, *A. niger*, *A. flavus*, and *F. oxysporum* (Fig. 9). The impact on colony colour and duration of conidia formation was observed and found to be affected by the BS-$Ag_2O$ NPs. The inhibitory effect of BS-$Ag_2O$ NPs on the mycelial growth of various tested fungi, namely *A. alternata*, *A. flavus*, and *A. niger*, was higher in comparison to *F. oxysporum*. At a concentration of 1.5 mg $mL^{-1}$ BS-$Ag_2O$ NPs, the percent inhibition was 91.70 ± 1.7, 62.65 ± 1.8, 58.96 ± 3.5 and 50.45 ± 1.5 on the growth of *A. alternata*, *A. flavus*, *A. niger*, and *F. oxysporum*, respectively. Decreasing the concentration of NPs to 0.5 mg $mL^{-1}$ resulted in percentage inhibition of 79.78 ± 1.5, 24.11 ± 2.3, 45.87 ± 5.2, and 35.70 ± 0.9 on the mycelial growth of phytopathogenic fungi. The fungitoxicity effect of BS-$Ag_2O$ against *F. oxysporum* was found to be minimum in comparison to *A. alternata*, *A. flavus* and *A. niger*. The maximum percent inhibition (91.70 ± 1.7) on the mycelial growth of *A. alternata* was observed at a concentration of 1.5 mg $mL^{-1}$. This was followed by *A. flavus* (62.65 ± 1.8), *A. niger* (58.96 ± 3.5), and *F. oxysporum* (50.45 ± 1.5). The decrease in the concentration of

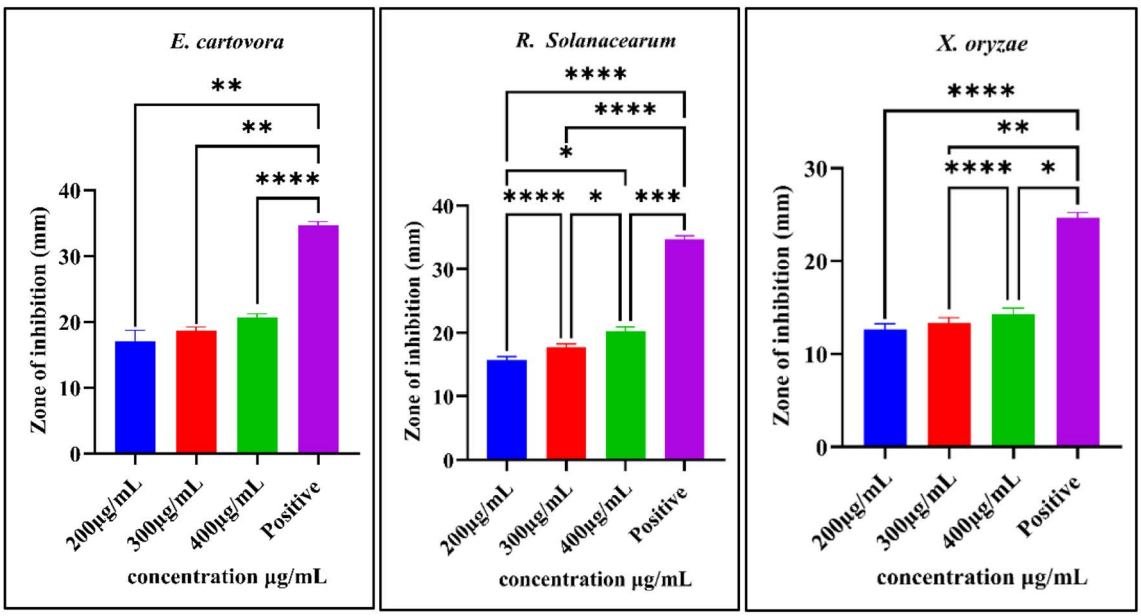


Fig. 7 Zone of inhibition (mm) against the growth of bacteria. Asterisks (*, **, ***, and ****) indicate significance levels ($P < 0.05$, 0.01, 0.001, and 0.0001) based on one-way ANOVA.

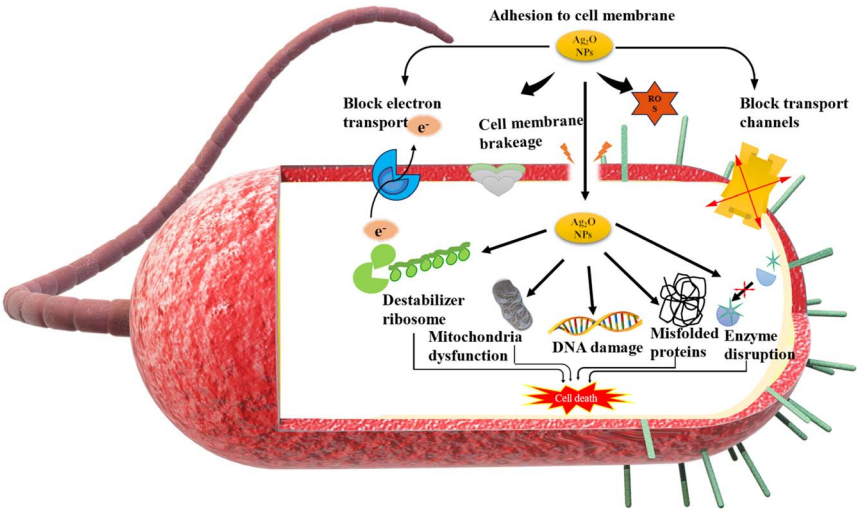


Fig. 8 Schematic presentation of a possible mechanism of antibacterial action of BS-$Ag_2O$ NPs.

nanoparticles resulted in a corresponding decrease in the percentage inhibition of mycelium growth. BS-$Ag_2O$ NPs-treated plate showed a change in the colour, shape, texture, form, and density of the fungal colony in comparison to untreated ones.[49]

Balashanmugam*et al.* (2016) also showed that the growth of three phytopathogenic fungi, *F. oxysporum*, *R. solani*, and *Curvularia* sp., as well as five human pathogenic fungi, *A. fumigatus*, *A. flavus*, *A. niger*, *Candida albicans*, and *Penicillium* sp., was significantly inhibited by green-synthesized Ag NPs.[50] Talie *et al.* (2020) reported 69.10% and 77.32% inhibition on the mycelial growth of *A. alternata* and *A. niger*, respectively, using Ag NPs.[51] The biosynthesized Ag NPs showed 81% mycelial

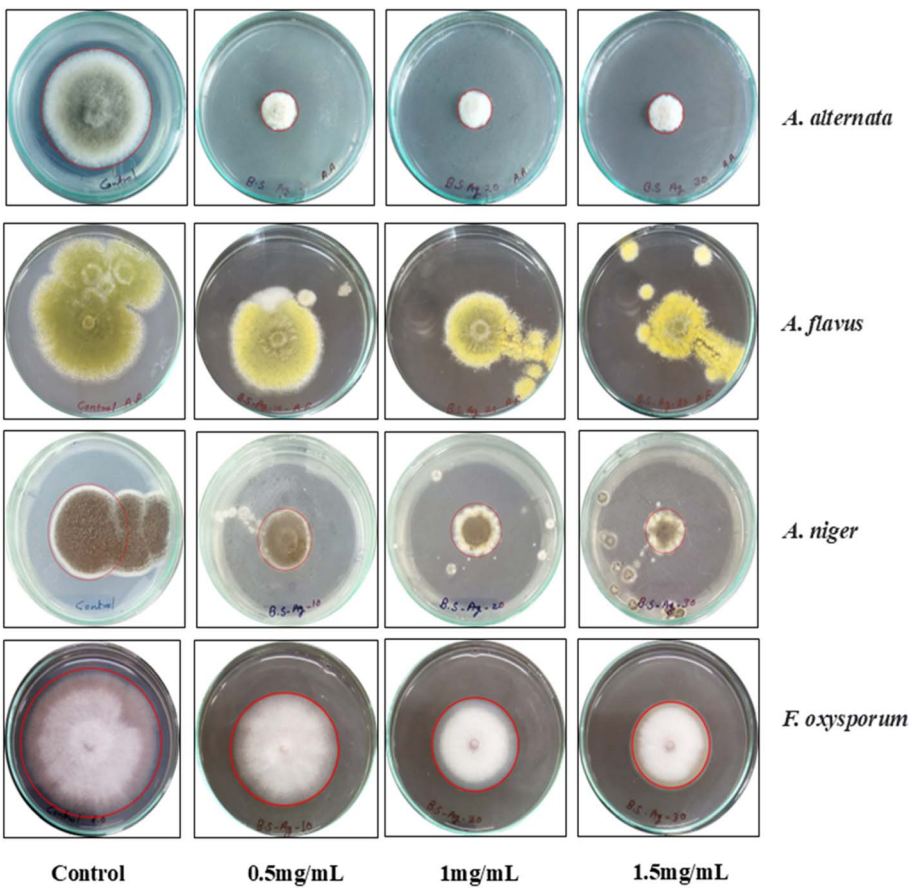


Fig. 9 Antifungal activity of BS-$Ag_2O$ NPs against phytopathogenic fungi at different concentrations.

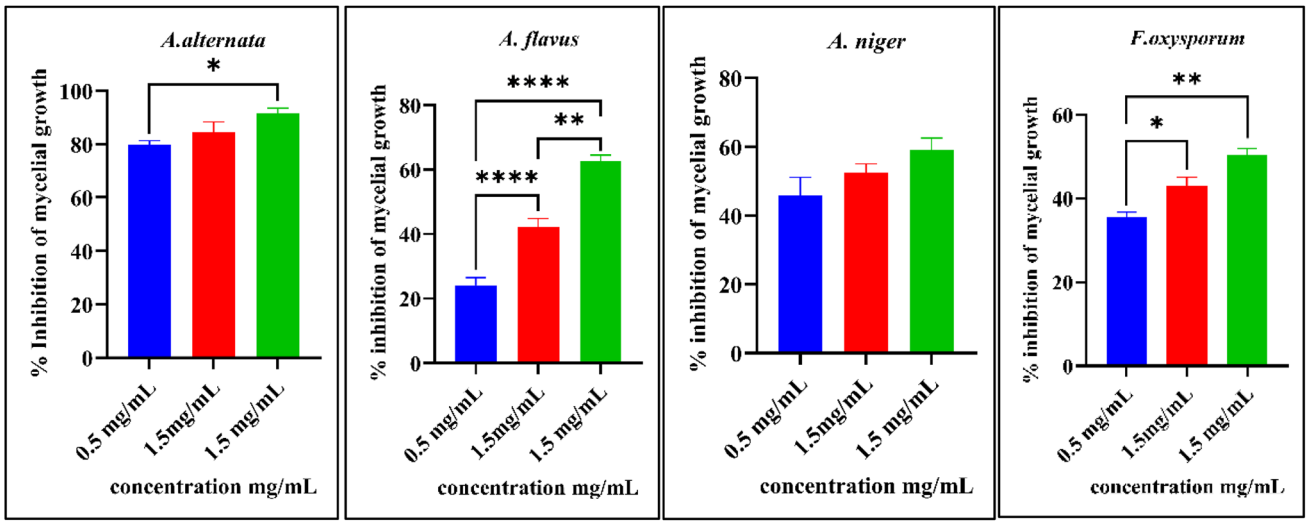


Fig. 10 Percentage inhibition on mycelial growth of phytopathogenic fungi by NPs. Asterisks (*, **, ***, and ****) indicate significance levels at $P < 0.05$, 0,01, 0.001 and 0.0001, respectively, based on one-way ANOVA.

growth inhibition against *A. alternata*, suggesting possible antifungal action.[52] The possible mechanism involvement by which $Ag_2O$ NPs break down the membrane permeability barrier is that $Ag_2O$ NPs perturb the membrane lipid bilayers, causing the leakage of ions and other materials as well as forming pores and dissipating the electrical potential of the membrane interaction of $Ag_2O$ NPs with the membrane structure.[53] The $Ag_2O$ NPs exhibited potent antifungal effects against tested fungi, probably through destruction of membrane integrity; therefore, it was concluded that BS-$Ag_2O$ NPs have considerable antifungal activity, deserving further investigation for crop applications (Fig. 10).[54]

### 3.4. Antioxidant activity studies of BS-$Ag_2O$ NPs

The BS-$Ag_2O$ NPs were evaluated for their free radical scavenging capacity by *in vitro* DPPH and ABTS assays. The results obtained for free radical scavenging activity at different concentrations were used for calculating percentage scavenging activity (Fig. 11).

DPPH free radical scavenging activity of BS-$Ag_2O$ NPs was compared with that of the (standard) ascorbic acid. It was observed that the synthesized BS-$Ag_2O$ NPs had potential DPPH inhibition activity compared with the standard (ascorbic acid). The average percentage (93.80 ± 0.14) scavenging activity was obtained using a standard ascorbic acid (80 μg $mL^{-1}$) solution, whereas the NP scavenging activity (25.85 ± 0.36) was obtained using 80 μg $mL^{-1}$ BS-$Ag_2O$ NPs. On increasing the concentration of NPs, the antioxidant activity was found to be increased. Peddi *et al.* (2021) also observed that with an increased concentration of NPs, the antioxidant activity increased.[36]

The ABTS free radical scavenging activity of BS-$Ag_2O$ NPs was assessed in comparison to the standard ascorbic acid. The results showed that the synthesized BS-$Ag_2O$ NPs exhibited remarkable ABTS inhibition activity, comparable to the standard ascorbic acid. The average percentage scavenging activity for the standard ascorbic acid was determined to be 100 ± 0% at a concentration of 80 μg $mL^{-1}$, while the green-synthesized BS-$Ag_2O$ NPs showed a percentage scavenging activity of 40.28 ± 0.90% at the same concentration. It was observed that as the concentration of the synthesized NPs increased, the free radical scavenging activity also increased. The results from the findings of several free radical scavenging activity methods indicate that the green-synthesized nanoparticles have excellent potential. These nanoparticles' improved therapeutic qualities might be

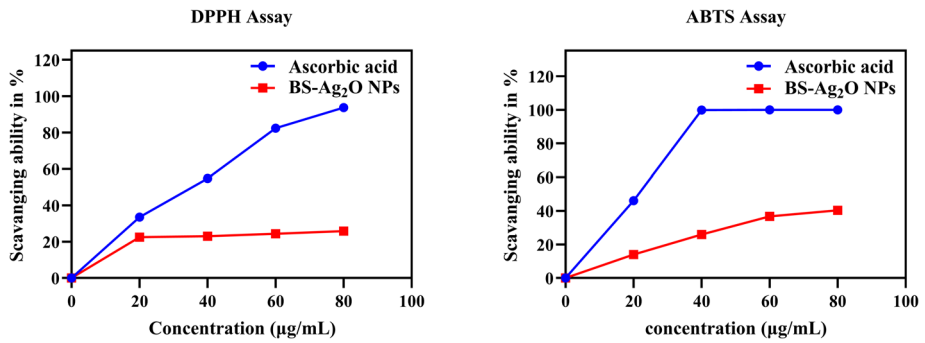


Fig. 11 DPPH and ABTS kinetic curves of biosynthesized BS-$Ag_2O$ NPs at different concentrations.

Table 2 Comparison of efficiency of $Ag_2O$ NPs and other nanoparticles

| Green-synthesized NPs | | | | | | |
|---|---|---|---|---|---|---|
| Nanoparticles | Plants | NP size range (nm) | Antibacterial activities | Antifungal activities | Antioxidant activities | References |
| Ag NPs | *Morus nigra* | 4–8 | — | *F. oxysporum*<br>*F. flavus*<br>*A. terrus*<br>*F. verticillioides* | — | 57 |
| Ag NPs | *Juniperus procera* | — | — | *A. fumigatus*<br>*F. chlamydosporum* | — | 58 |
| Ag and $Ag_2O$ NPs | *Aloe vera* | 10–70 | *E. coli*<br>*S. aureus* | — | — | 59 |
| $Ag_2O$ NPs | *Zephyranthes Rosea* flower | 10–30 | *E. coli*<br>*S. aureus*<br>*Streptococcus mutans* | | DPPH | 60 |
| $Ag_2O$ NPs | *Mentha pulegium*<br>*Ficus carica* | 9–100 | | *C. albicans* and *A. oryzae* | DPPH<br>ABTS | 30 |
| Cu NPs | *Ageratum houstonianum* Mill. | ~80 | *E. coli* | — | — | 61 |
| Au NPs | *Ziziphus zizphus* | 3 | *E. coli* | *C. albicans* | | 43 |
| Zn NPs | *Euphorbia hirta* | 20–25 | *S. mutans*<br>*S. aureus*<br>*Clostridium absonum*<br>*E. coli* | *Arthogrophis cuboida*<br>*Aspergillus fumigatus*<br>*A. niger* | — | 62 |
| $Ag_2O$ NPs | *B. sinuata* | 3–14 | *E. carotovora*<br>*R. solanacearum*<br>*X. oryzae* | *A. alternata*<br>*A. flavus*<br>*A. niger*<br>*F. oxysporum* | DPPH<br>ABTS | This study |

due to the highly bioactive chemical compound present in the BS plant extract utilized to create them.

The antioxidant activity is ascribed to numerous mechanisms, including chain inhibition prevention, transition metal ion catalyst binding, peroxide breakdown, hydrogen abstraction prevention, reductive capacity, and radical scavenging.[55] Free radicals are different chemical entities that contain one or more unpaired electrons. Due to their instability, they cause damage to other molecules' stability by removing their electron. They create highly reactive substances inside the system and can harm short-lived chemical species. The human body or other living organisms constantly produce these radicals because they need them for immune system function, chemical signalling, detoxification, and energy generation.[56] Furthermore, the antioxidant free radical response is a second order reaction, which is dependent on the quantity, chemical structure, medium, and reaction conditions. The primary source of phytochemical compounds' antioxidant activity is their redox properties, which can play a crucial role in absorbing and neutralizing free radicals as well as quenching singlet and triplet oxygens (Table 2).[37]

## 4. Conclusion

Green-synthesized BS-$Ag_2O$ NPs have a promising future due to their eco-friendly nature and easy synthesis process. The biogenic BS-$Ag_2O$ NPs have been synthesized using the plant extract of *Blumea sinuata* (Lour.) Merr. The analysis of phytochemicals of the plant extract showed the presence of tannins, flavonoids, quinones, phenols, terpenoids, cardiac glycosides, coumarins, anthraquinones, and steroids. Phytochemicals present in the plant extract might be responsible for active bioreduction and stabilization of $Ag_2O$ in the form of BS-$Ag_2O$ NPs. BS-$Ag_2O$ NPs were characterized using UV-visible spectroscopy, XRD, FTIR, DLS, zeta potential measurements and HRTEM-EDS. The BS-$Ag_2O$ NPs were found to have a crystalline nature and were nearly round in shape with an average particle size of 7.98 nm. BS-$Ag_2O$ NPs showed antibacterial effects against Gram-negative bacteria *E. carotovora*, *R. solanacearum*, and *X. oryzae* with remarkable zones of inhibition. The antifungal effect of biosynthesized BS-$Ag_2O$ NPs was assessed by determining the percentage of inhibition in the mycelial growth of fungi *A. alternata*, *A. niger*, *A. flavus*, and *F. oxysporum*, and the observation indicates remarkable inhibition in the growth of phytopathogenic fungi. Bio-fabricated BS-$Ag_2O$ NPs showed free radical scavenging characteristics. High antioxidant activity was recorded using DPPH and ABTS methods. The findings encourage antibacterial, antifungal, and antioxidant drug therapy research. BS-$Ag_2O$ NPs offer promising solutions for various agricultural challenges; their antimicrobial properties can help manage plant diseases, ultimately ensuring food security and environmental protection. Further research and development is recommended to optimize the application methods of NPs in agriculture, ensuring their efficiency and safety.

## Data availability

In case data are required, the authors shall be pleased to share all components of the experimental data as per the guidelines of this journal.

## Author contributions

This research work was carried out under the supervision of Prof. A. K. Shukla and Dr S. Mallick. Mr Umakant Pradhan, Mr J. P. Prajapati, Mr P. Majhi, Ms D. Sahu and Mr Rajesh Kumar Singh were associated with the methodology and experimental work. The manuscript was prepared by Mr Umakant Pradhan and Mr J. P. Prajapati. Prof. A. K. Shukla and Dr S. Mallick supervised, reviewed and edited the manuscript.

## Conflicts of interest

The authors declare no conflict of financial and academic interest.

## Acknowledgements

This is to certify that we have not received a grant from any funding agency to carry out this research work. The present investigation was conceptualized by us and the existing lab facility was used to pursue the research work.

## References

1 M. Gomathi, A. Prakasam, P. V. Rajkumar, S. Rajeshkumar, R. Chandrasekaran and P. M. Anbarasan, Green synthesis of silver nanoparticles using Gymnema sylvestre leaf extract and evaluation of its antibacterial activity, *S. Afr. J. Chem. Eng.*, 2020, **32**, 1–4.

2 P. Hemlata, R. Meena, A. P. Singh and K. K. Tejavath, Biosynthesis of Silver Nanoparticles Using Cucumis prophetarum Aqueous Leaf Extract and Their Antibacterial and Antiproliferative Activity against Cancer Cell Lines, *ACS Omega*, 2020, **5**, 5520–5528.

3 P. N. Mahlambi and M. J. Moloto, Starch-capped silver oxide (Ag2O) nanoparticles: synthesis, characterization and antibacterial activity, *Dig. J. Nanomater. Biostruct.*, 2022, **17**, 921–930.

4 S. Mallick, P. Sanpui, S. S. Ghosh, A. Chattopadhyay and A. Paul, Synthesis, characterization and enhanced bactericidal action of a chitosan supported core-shell copper-silver nanoparticle composite, *RSC Adv.*, 2015, **5**, 12268–12276.

5 K. Elankathirselvan, P. Paunkumar, K. Srinivasan, T. Premkumar and S. G. Babu, Green synthesis and structural and cytotoxic properties of a new silver(I) complex: Solid-state, single-source precursor of Ag and Ag2O NPs, *J. Mol. Struct.*, 2023, **1301**, 137298.

6 C. Tanase, L. Berta, N. A. Coman, I. Roşca, A. Man, F. Toma, A. Mocan, L. Jakab-Farkas, D. Biró and A. Mare, Investigation of *in vitro* antioxidant and antibacterial potential of silver nanoparticles obtained by biosynthesis using beech bark extract, *Antioxidants*, 2019, **8**(10), 459.

7 H. Dabhane, S. Ghotekar, P. Tambade, S. Pansambal, H. C. A. Murthy, R. Oza and V. Medhane, A review on environmentally benevolent synthesis of CdS nanoparticle and their applications, *J. Environ. Chem. Ecotoxicol.*, 2021, **3**, 209–219.

8 Y. Kashid, S. Ghotekar, M. Bilal, S. Pansambal, R. Oza, R. S. Varma, V. H. Nguyen, H. C. Ananda Murthy and D. Mane, Bio-inspired sustainable synthesis of silver chloride nanoparticles and their prominent applications, *J. Indian Chem. Soc.*, 2022, **99**, 100335.

9 N. M. Noah and P. M. Ndangili, Green synthesis of nanomaterials from sustainable materials for biosensors and drug delivery, *Sens Int.*, 2022, **3**, 100166.

10 K. Neme, A. Nafady, S. Uddin and Y. B. Tola, Application of nanotechnology in agriculture, postharvest loss reduction and food processing: food security implication and challenges, *Heliyon*, 2021, **7**, e08539.

11 E. Takele Assefa, G. Shumi, K. Mohammed Gendo, G. Kenasa and N. Roba, Review on green synthesis, characterization, and antibacterial activity of CuO nanoparticles using biomolecules of plants extract, *Results Chem.*, 2024, **8**, 101606.

12 P. Selvam, S. Antharjanam, K. Srinivasan and T. Premkumar, "A 1D silver(I) coordination polymer of a new hydrozone-hydrazide ligand: Spectral, structural, emission, and antibacterial properties and its application as a solid source precursor for silver oxide nanoparticles", *J. Phys. Chem. Solids*, 2021, **160**, 110368.

13 M. Nakano, T. Fujiwara and N. Koga, Thermal Decomposition of Silver Acetate: Physico-Geometrical Kinetic Features and Formation of Silver Nanoparticles, *J. Phys. Chem. C*, 2016, **120**, 8841–8854.

14 S. Haq, K. A. Yasin, W. Rehman, M. Waseem, M. N. Ahmed, M. I. Shahzad, N. Shahzad, A. Shah, M. U. Rehman and B. Khan, Green Synthesis of Silver Oxide Nanostructures and Investigation of Their Synergistic Effect with Moxifloxacin Against Selected Microorganisms, *J. Inorg. Organomet. Polym. Mater.*, 2021, **31**, 1134–1142.

15 F. C. Kenechukwu, K. C. Ugwu, C. S. Offorbuike, E. M. Ojukwu, T. H. Gugu, R. E. Eze and &A. A. Attama, Solidified reverse micellar solution-based chitosan-coated solid lipid nanoparticles as a new approach to enhance oral delivery of artemether in malaria treatment, *BMC Chem.*, 2025, **19**(1), 1–25.

16 A. Dandia, S. Bansal, R. Sharma, K. S. Rathore and V. Parewa, Microwave-assisted nanocatalysis: A CuO NPs/rGO composite as an efficient and recyclable catalyst for the Petasis-borono-Mannich reaction, *RSC Adv.*, 2018, **8**, 30280–30288.

17 F. Bamiduro, N. William, N. Hondow, S. Milne, A. Nelson and R. Drummond-Brydson, Hydrothermal Synthesis of Silver Nanoparticles for High Throughput Biosensing Applications, *MRS Adv.*, 2018, **3**, 861–866.

18 Y. Dasaradhudu and M. Arunachalam Srinivasan, "Synthesis and characterization of silver nano particles using co-precipitation method", *Mater. Today: Proc.*, 2020, **33**, 720–723.

19 M. Barwant, Y. Ugale, S. Ghotekar, P. Basnet, V. H. Nguyen, S. Pansambal, H. C. Ananda Murthy, M. Sillanpaa, M. Bilal, R. Oza and V. Karande, Eco-friendly synthesis and

characterizations of Ag/AgO/Ag2O nanoparticles using leaf extracts of Solanum elaeagnifolium for antioxidant, anticancer, and DNA cleavage activities, *Chem. Pap.*, 2022, **76**, 4309–4321.

20 A. Chauhan, G. Rana, V. Dutta, A. Kumari, S. Krishna Rao, R. Subbarayan, K. Ravi, S. Selvaraj and S. Ghotekar, Recent trends in phyto-mediated iron-based nanomaterials for environmental remediation and biomedical applications, *Inorg. Chem. Commun.*, 2024, **160**, 111976.

21 D. Garibo, H. A. Borbón-Nuñez, J. N. D. de León, E. García Mendoza, I. Estrada, Y. Toledano-Magaña, H. Tiznado, M. Ovalle-Marroquin, A. G. Soto-Ramos, A. Blanco, J. A. Rodríguez, O. A. Romo, L. A. Chávez-Almazán and A. Susarrey-Arce, Green synthesis of silver nanoparticles using Lysiloma acapulcensis exhibit high-antimicrobial activity, *Sci. Rep.*, 2020, **10**, 1–11.

22 V. Kumar, D. K. Singh, S. Mohan, D. Bano, R. K. Gundampati and S. H. Hasan, Green synthesis of silver nanoparticle for the selective and sensitive colorimetric detection of mercury (II) ion, *J. Photochem. Photobiol., B*, 2017, **168**, 67–77.

23 M. G. Agidew, Phytochemical analysis of some selected traditional medicinal plants in Ethiopia, *Bull. Natl. Res. Cent.*, 2022, **46**, 1.

24 L. Flores-Bocanegra, E. E. González-Hernández, A. Soto-Sosa, M. E. González-Trujano and &S. Cristians, Phytochemical analysis and evaluation of the inhibitory effect of the Cunila lythrifolia Benth aerial parts on abdominal pain and some digestive enzymes, *J. Ethnopharmacol.*, 2025, **337**, 118991.

25 J. Fowsiya and G. Madhumitha, Biomolecules derived from Carissa edulis for the microwave assisted synthesis of Ag 2 O nanoparticles: A study against S. incertulas, C. medinalis and S. mauritia, *J. Cluster Sci.*, 2019, **30**, 1243–1252.

26 J. Mussin, V. Robles-Botero, R. Casañas-Pimentel, F. Rojas, L. Angiolella, E. San Martín-Martínez and G. Giusiano, Antimicrobial and cytotoxic activity of green synthesis silver nanoparticles targeting skin and soft tissue infectious agents, *Sci. Rep.*, 2021, **11**, 1–13.

27 N. Liaqat, N. Jahan, Khalil-ur-Rahman, T. Anwar and H. Qureshi, Green synthesized silver nanoparticles: Optimization, characterization, antimicrobial activity, and cytotoxicity study by hemolysis assay, *Front. Chem.*, 2022, **10**, 1–13.

28 A. Sobhani-Nasab and M. Behpour, Synthesis and characterization of AgO nanostructures by precipitation method and its photocatalyst application, *J. Mater. Sci.:Mater. Electron.*, 2016, **27**, 1191–1196.

29 N. El Messaoudi, A. El Mouden, Y. Fernine, M. El Khomri, A. Bouich, N. Faska, Z. Ciğeroğlu, J. H. P. Américo-Pinheiro, A. Jada and A. Lacherai, Green synthesis of Ag2O nanoparticles using Punica granatum leaf extract for sulfamethoxazole antibiotic adsorption: characterization, experimental study, modeling, and DFT calculation, *Environ. Sci. Pollut. Res.*, 2023, **30**, 81352–81369.

30 M. Shahzad Shirazi, M. Moridi Farimani, A. Foroumadi, K. Ghanemi, M. Benaglia and P. Makvandi, Bioengineered synthesis of phytochemical-adorned green silver oxide (Ag2O) nanoparticles *via* Mentha pulegium and Ficus carica extracts with high antioxidant, antibacterial, and antifungal activities, *Sci. Rep.*, 2022, **12**, 1–15.

31 T. M. Hoi, P. Satyal, L. T. Huong, D. V. Hau, T. D. Binh, D. T. H. Duyen, D. N. Dai, N. G. Huy, H. Van Chinh, V. Van Hoa, N. H. Hung and W. N. Setzer, Essential Oils from Vietnamese Asteraceae for Environmentally Friendly Control of Aedes Mosquitoes, *Molecules*, 2022, **27**, 1–16.

32 Y. Peng, X. Pu, Q. Yu, H. Zhou, T. Huang, B. Xu and X. Gao, Comparative Pollen Morphology of Selected Species of Blumea DC. and Cyathocline Cass. and Its Taxonomic Significance, *Plants*, 2023, **12**, 16.

33 P. P. Hazra, B. Mondal, D. Das, P. Majhi, U. Pradhan, S. Mallick, A. K. Shukla, R. K. Das and U. K. Roy, Multicomponent consecutive Barbier propargylation and CuAAC click reactions using Zn/CuFe2O4 reagent: Entry to anti-fungal triazole compounds, *Tetrahedron*, 2023, **139**, 133442.

34 S. Renganathan, S. Subramaniyan, N. Karunanithi, P. Vasanthakumar, A. Kutzner, P. S. Kim and K. Heese, Antibacterial, antifungal, and antioxidant activities of silver nanoparticles biosynthesized from Bauhinia tomentosa Linn, *Antioxidants*, 2021, **10**, 12.

35 M. Todorova, A. Kosateva, V. Petrova, B. Ranguelov, S. Atanasova-Vladimirova, G. Avdeev, I. Stoycheva, E. Pisareva, A. Tomova, L. Velkova, A. Dolashki and P. Dolashka, Green Synthesis of Antibacterial CuO Nanoparticles Based on the Synergy Between Cornu aspersum Snail Mucus and Ascorbic Acid, *Molecules*, 2025, **30**, 1–25.

36 P. Peddi, P. R. Ptsrk, N. U. Rani and S. L. Tulasi, Green synthesis, characterization, antioxidant, antibacterial, and photocatalytic activity of Suaeda maritima (L.) Dumort aqueous extract-mediated copper oxide nanoparticles, *J. Genet. Eng. Biotechnol.*, 2021, **19**, 1.

37 D. Rehana, D. Mahendiran, R. S. Kumar and A. K. Rahiman, Evaluation of antioxidant and anticancer activity of copper oxide nanoparticles synthesized using medicinally important plant extracts, *Biomed. Pharmacother.*, 2017, **89**, 1067–1077.

38 M. S. Jadhav, S. Kulkarni, P. Raikar, D. A. Barretto, S. K. Vootla and U. S. Raikar, Green biosynthesis of CuO & Ag-CuO nanoparticles from Malus domestica leaf extract and evaluation of antibacterial, antioxidant and DNA cleavage activities, *New J. Chem.*, 2018, **42**, 204–213.

39 S. O. Oselusi, N. R. S. Sibuyi, M. Meyer, S. Meyer and A. M. Madiehe, Phytofabrication of silver nanoparticles using Ehretia rigida leaf aqueous extract, their charactrization, antioxdent and antimicrobial activities, *Mater. Today Sustain.*, 2025, **29**, 101059.

40 J. Prasad Prajapati, A. Toppo, P. Majhi, U. Pradhan, A. Das, D. Das, G. Sriramulu, S. Mallick, S. Katlakunta and A. K. Shukla, Biogenic Synthesis, Characterization, and Antifungal Activity Studies of Copper Oxide Nanoparticles Using Aqueous Extract of Moringa oleifera Leaves, *ChemistrySelect*, 2023, **8**, 34.

41 S. K. Sahu, A. Kushwaha, U. Pradhan, P. Majhi, A. K. Shukla and T. K. Ghorai, Sustainable green synthesis of Hedychium coronarium leaf extract-stabilized silver nanoparticles and their applications: colorimetric sensing of Sn2+ and Hg2+ and antifungal and antimicrobial properties, *Nanoscale Adv.*, 2024, **6**(21), 5361–5374.

42 D. Sun, R. Chen, L. Lei and F. Zhang, Green synthesis of silver nanoparticles from the endophytic fungus Panax notoginseng and their antioxidant and antimicrobial activities and effects on cherry tomato preservation, *Int. J. Food Microbiol.*, 2025, **431**, 111083.

43 A. A. A. Aljabali, Y. Akkam, M. S. Al Zoubi, K. M. Al-Batayneh, B. Al-Trad, O. A. Alrob, A. M. Alkilany, M. Benamara and D. J. Evans, Synthesis of gold nanoparticles using leaf extract of ziziphus zizyphus and their antimicrobial activity, *Nanomaterials*, 2018, **8**, 1–15.

44 M. A. Arenas Garica, S. Hidouri, X. Hao, J. M. deMedeiros Dantas and N. M. Dorval Courchesne, Biological Synthesis of Reusable Silver Nanoparticle-Protein Antimicrobial Films, *Adv. Mater. Interfaces*, 2025, 202400649.

45 N. Kimta, S. Puri, A. Kumari, R. Verma, R. Sharma, K. A. Khan, K. T. Chen and D. Kumar, Applications of Pteridophytes in Nanotechnology: a class that has not yet explored to the extent of its potential, *Green Chem. Lett. Rev.*, 2025, **18**, 1–24.

46 A. Abbas, S. S. Naz and S. A. Syed, Antimicrobial activity of silver nanoparticles (AgNPs) against Erwinia carotovora subsp. atroseptica & Alternaria alternata, *Pakistan J. Agric. Sci.*, 2019, **56**, 113–117.

47 B. Javed, A. Nadhman and Z. U. R. Mashwani, Optimization, characterization and antimicrobial activity of silver nanoparticles against plant bacterial pathogens phyto-synthesized by Mentha longifolia, *Mater. Res. Express*, 2020, **7**, 8.

48 S. Dilbar, H. Sher, H. Ali, R. Ullah, A. Ali and Z. Ullah, Antibacterial Efficacy of Green Synthesized Silver Nanoparticles Using Salvia nubicola Extract against Ralstonia solanacearum, the Causal Agent of Vascular Wilt of Tomato, *ACS Omega*, 2023, **8**, 31155–31167.

49 S. W. Kim, K. S. Kim, K. Lamsal, Y. J. Kim, S. Bin Kim, M. Jung, S. J. Sim, H. S. Kim, S. J. Chang, J. K. Kim and Y. S. Lee, An *in vitro* study of the antifungal effect of silver nanoparticles on oak wilt pathogen Raffaelea sp, *J. Microbiol. Biotechnol.*, 2009, **19**, 760–764.

50 P. Balashanmugam, M. D. Balakumaran, R. Murugan, K. Dhanapal and P. T. Kalaichelvan, Phytogenic synthesis of silver nanoparticles, optimization and evaluation of *in vitro* antifungal activity against human and plant pathogens, *Microbiol. Res.*, 2016, **192**, 52–64.

51 M. D. Talie, A. Hamid Wani, N. Ahmad, M. Yaqub Bhat and J. Mohd War, Green syntheis of silver nanoparticles (AgNPs) using Helvella leucopus pers. and their antimycotic activity against fungi causing fungal rot of apple, *Asian J. Pharm.*, 2020, 161–165.

52 A. Dashora, K. Rathore, S. Raj and K. Sharma, Synthesis of silver nanoparticles employing Polyalthia longifolia leaf extract and their *in vitro* antifungal activity against phytopathogen, *Biochem. Biophys. Rep.*, 2022, **31**, 101320.

53 C. C. Achilonu, T. Ramatla, M. Maleke, P. Kumar, O. A. Igbalajobi and C. B. Noel, Potential Influence of Antifungal-drug Resistant Pathogens in Patients with Cholangiocarcinoma and the Application of Nanoparticle Mechanisms as Novel Antifungal and Anticancer Agents, *Curr. Clin. Microbiol. Rep.*, 2025, **12**(1), 1–10.

54 H. S. Al-Jobory, K. M. A. Hasan and A. F. Alkaim, Antifungal effect of silver nanoparticles on dermatophytes isolated from clinicalspecimens, *Plant Arch.*, 2020, **20**, 2897–2903.

55 O. Sabira, A. P. Ajaykumar, S. R. Varma, K. N. Jayaraj, M. Kotakonda, P. Kumar, P. Vaikkathillam, V. Sivadasan Binitha, A. P. Alen, A. V. Raghu and K. V. Zeena, Nepenthes pitcher fluid for the green synthesis of silver nanoparticles with biofilm inhibition, anticancer and antioxidant properties, *Sci. Rep.*, 2025, **15**, 1–20.

56 Z. Yuksekdag, R. Kilickaya, F. Kara and B. C. Acar, Biogenic-Synthesized Silver Nanoparticles Using the Ligilactobacillus salivarius KC27L Postbiotic: Antimicrobial, Anti-Biofilm, and Antioxidant Activity and Cytotoxic Effects, *Probiotics Antimicrob. Proteins*, 2025, 1–15.

57 R. A. Hafez, M. A. Abdel-Wahhab, A. F. Sehab and A. Z. A. K. El-Din, Green synthesis of silver nanoparticles using Morus nigra leave extract and evaluation their antifungal potency on phytopathogenic fungi, *J. Appl. Pharm.*, 2017, 041–048.

58 M. M. Bakri, M. A. El-Naggar, E. A. Helmy, M. S. Ashoor and T. M. Abdel Ghany, Efficacy of Juniperus procera Constituents with Silver Nanoparticles Against Aspergillus fumigatus and Fusarium chlamydosporum, *Bionanoscience*, 2020, **10**, 62–72.

59 N. S. Flores-Lopez, J. A. Cervantes-Chávez, D. G. Téllez de Jesús, M. Cortez-Valadez, M. Estévez-González and R. Esparza, Bactericidal and fungicidal capacity of Ag2O/Ag nanoparticles synthesized with Aloe vera extract, *J. Environ. Sci. Health, Part A: Toxic/Hazard. Subst. Environ. Eng.*, 2021, **56**, 762–768.

60 G. Maheshwaran, A. Nivedhitha Bharathi, M. Malai Selvi, M. Krishna Kumar, R. Mohan Kumar and S. Sudhahar, Green synthesis of Silver oxide nanoparticles using Zephyranthes Rosea flower extract and evaluation of biological activities, *J. Environ. Chem. Eng.*, 2020, **8**, 104137.

61 S. K. Chandraker, M. Lal, M. K. Ghosh, V. Tiwari, T. K. Ghorai and R. Shukla, Green synthesis of copper nanoparticles using leaf extract of Ageratum houstonianum Mill. and study of their photocatalytic and antibacterial activities, *Nano Express*, 2020, **2**, 53–63.

62 W. Ahmad and D. Kalra, Green synthesis, characterization and anti microbial activities of ZnO nanoparticles using Euphorbia hirta leaf extract, *J. King Saud Univ., Sci.*, 2020, **32**, 2358–2364.